Available online at www.sciencedirect.com

ScienceDirect

Procedia Engineering 175 (2017) 332 – 340

Procedia Engineering

www.elsevier.com/locate/procedia

1st International Conference on the Material Point Method, MPM 2017

Novel procedure to validate MPM results by means of PIV measurements

Núria Pinyol[a,b,*], Mauricio Alvarado[a,b], Ferran Parera[a], Alba Yerro[c]

[a]*Universitat Politècnica de Catalunya, Barcelona (UPC), Barcelona Spain*
[b]*Centre Internacional de Mètodes Numèrics en Enginyeria (CIMNE), Barcelona, Spain*
[c]*University of Cambridge, Cambridge, UK*

Abstract

The Particle Image Velocimetry is a powerful non-invasive technique to analyse displacements in experimental tests. Displacement increments elapsed between the capture of two digital images are commonly measured on points of a predefined grid fixed in the space. Therefore, tracking the movement of physical particles, which is interesting information especially in cases dealing with large displacements, is not possible when using this procedure. A post-processing code has been developed to get accumulated displacements, incremental and accumulated strains, as well as other variables such as velocity and acceleration, in points that represent a portion of the deformable object analysed. The procedure is of interest specially when dealing with large displacements. The method presented is especially useful to compare experimental measurements with MPM numerical results. The variables from the numerical model stored in material points can be directly compared with the experimental measurements obtained by means of the post-process code presented in the paper. The methodology is applied for the analysis of the failure of a dry granular slope performed in a 1g scaled laboratory test which is numerically modelled with an MPM code (GeoPart). The aim of the paper is to show the capabilities of the new PIV interpretation procedure by comparing experimental and numerical results. The accuracy of the MPM model presented is not the main focus of the paper, but some limitations of the model are highlighted.

Peer-review under responsibility of the organizing committee of the 1st International Conference on the Material Point Method

Keywords: particle image velocimetry; strain, displacements; velocity, laboratory measuments; material point method.

* Corresponding author.
E-mail address: nuria.pinyol@upc.edu

Peer-review under responsibility of the organizing committee of the 1st International Conference on the Material Point Method
doi:10.1016/j.proeng.2017.01.039

1. Introduction

Particle Image Velocimetry is a non-invasive technique to measure displacements in experimental tests by means of the comparison of pairs of digital images of a deformable object in an interval time (Δt). Comparison of images is performed by techniques of Digital Image Correlation (DIC). The differences observed between the first and the second image are evaluated to obtain a set of relative displacement vectors associated with points of the observed object. PIV was firstly developed by Adrian [1] to evaluate the movement in fluids. In geotechnics, White et al. [2] applied this technique to measure displacement in soils and developed software (GeoPIV) to process the images. Take et al. [3] used this technique to analyse landslides in reduced-scale models and Take and Bolton [4] focused on the slope failures in clays tested in a centrifuge. Other applications of PIV technique have been presented by Gilbert et al.[5], Niedostatkiewicz et al. [6] and Senatore et al. [7]. A description of DIC and a review of the different methodologies used are presented by Pan et al.[8] and more recently by Take [9].

The basis of the procedure is to process the digital images and to encode them in patterns of pixels (Fig. 1). The area of interest of the image taken at t_1, reference image, is divided in a mesh of interrogation sub-areas also called patches. The code analyses the geometrical and colour patterns of each sub-area of this image and searches its corresponding counterpart in the image taken at t_2. The search-area extends a predefined distance S_{max} beyond the initial interrogation area. This procedure is performed for all sub-areas of interrogation of the reference image to evaluate the whole image. The result is the localization of all the referred patches in the deformed image (taken at time t_2) by means a correlation procedure.

Fig. 1. Ideal example of a codification in patterns in the PIV technique. (a) digital picture; (b) simplified gray scaled picture; (c) binary code.

Comparing the position of each patch in correlated images, the displacement increment vector field elapsed during an interval time Δt is obtained. Figure 2 shows the displacement vector field obtained in a scaled laboratory experiment. Red crosses in the figure indicate the zone out of the area of interest.

This procedure is applied at different times to evaluate the motion of the object in time. The correlation between the deformed image and the first one has a clear limit due to mismatch in regions experiencing large deformations. For this reason, when dealing with large displacements, the reference image should be updated. The common procedure is to select a time interval between images that allows a proper correlation and the measurement of the "instantaneous" displacements occurred during the time interval and the reference image is updated for each time step.

Several techniques can be applied in the measurement of displacements. One option is based on measuring displacements in a set of points fixed in the space which correspond to the centres of the patches initially defined (Eulerian approach). As a consequence, the tracking of a given particle of the object during the motion is not directly obtained. The accumulated displacements cannot be calculated as the sum of the measured displacements since they are measured in fixed points in the space instead of being measured in points attached to the observed object.

Notice that the image analysed by means of PIV (an example is given in Figure 2) provides information about the accumulated displacement since the photograph provides the deformed geometry of the object. However, this information is not available quantitatively by means of PIV techniques evaluated in Eulerian mode. Only instantaneous displacement elapsed during an interval time are directly obtained

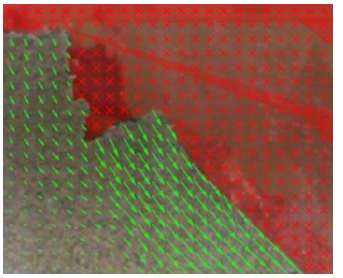

Fig. 2. Displacement vector field.

A numerical tool to calculate the accumulated displacements of points attached to the observed object from the instantaneous displacements calculated on points fixed in the space by means of PIV technique has been developed by Pinyol and Alvarado [10]. The methodology is inspired in the MPM that combine two spatial discretizations: Eulerian (fixed reference points in the space) and Lagrangian (moving reference point attached to the material). The methodology is of special interest in the calculation of strains in cases involving large displacements.

The procedure is applied to a 1g scaled laboratory experiment in which the failure of a dry sandy slope is induced in a transparent box (1000 cm long and 200 cm wide) and the processed measurements are compared with MPM results. The slope motion was recorded using a reflex camera capable of taking pictures at a frame rate of 50 fps which enables to capture the movement of the slope. The experiment is described below.

The images recording the slide motion were analysed by means of the free-commercial software PIVLab [11] developed at the Groningen University (Netherlands). The PIV measurements were post-processed by means of the procedure presented here. Accumulated displacements, strains and accumulated strains, velocity and acceleration are evaluated. This experimental data is finally compared with the numerical results calculated with a 2D MPM code, GeoPart [12],[13].

2. Method explanation

The post-processing code developed is able to calculate the displacements associated with physical particles from the displacement measured by PIV in points fixed in the space. It is assumed that the data provided by PIV is: (a) the time interval Δt elapsed between image capturing; (b) the coordinates of each center of the rectangular grid where displacement is measured; and (c) the corresponding displacement increments, $\boldsymbol{u}(t)$ at each center of the rectangular grid. Once displacements occurred in each time step are assigned to the physical particles, accumulated displacements and strains can be calculated.

The procedure involves the following steps inspired on the Material Point Method theory:

- The centres of patches where displacements are measured by PIV are selected as nodes of a 2D rectangular mesh.
- The elements filled or partially filled by the analysed material should be identified.
- A set of material points is defined in each element of the mesh filled or partially filled by the analysed material.
- The time interval (Δt) between images, the inverse of the fps of the video, is defined as the calculation time in the standard MPM calculation.
- At each time step, the instantaneous displacement measured in PIV should be assigned to the nodes of the rectangular mesh.
- At each time step displacements are mapped to the material points using the shape functions.
- Strain increments are calculated at material points following MPM techniques.
- Accumulated displacement and strains are mapped to the material points.
- The position of the material points is updated.
- Return to step 5 to begin a new time step of calculation.

3. Example of application

3.1. Description of the case study

The case study is the failure and run-out of a 60° sand slope in dry conditions (at water content in equilibrium at the relative humidity of the laboratory). The granular soil is a calcareous-siliceous sand from Castelldefels beach (Catalonia, Spain). The slope was built in a transparent and instrumented box designed to simulated slope failures under relative humidity control. The design allows the inflow of water from both the bottom and the top of the box. The slope dimensions are 250mm height, 200mm width and 330mm long (Figure 3). In the case presented here, the slope is initially stable because an inclined guillotine is restraining the motion. Failure is triggered by removing this guillotine. The motion lasts 0.5 seconds and the final stable geometry is shown in Figure 3b.

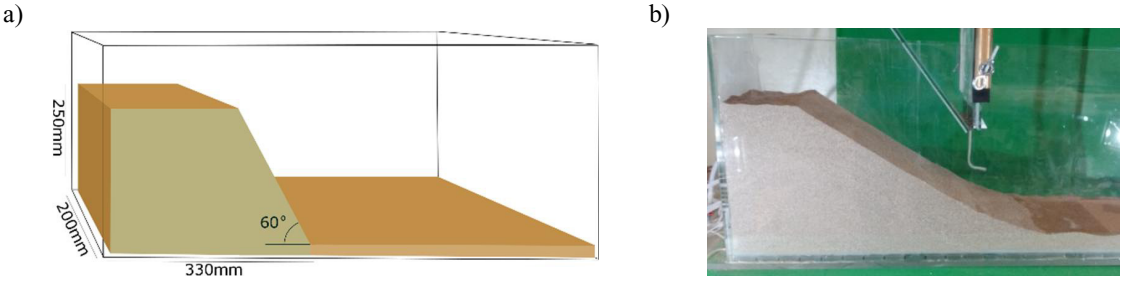

Fig. 3. (a) Diagram of the selected case study; (b) Photograph of the slope at equilibrium after failure.

The test was recorded in a 50 fps FullHD video using a reflex camera with shutter manual control. Recorded digital images of the failure and postfailure behaviour of the slope were analysed by means of PIVLab software [11]. A sequential scheme was selected to correlate each image with the previous one. Quadrilateral patches of 0.0075 x 0.0075 m were selected for the analysis.

3.2. PIV and post-processed measurements

Figure 4a shows the instantaneous velocity measured by PIV at three different times. The grid of patches centres is indicated by red crosses. The equivalent instantaneous velocity field plotted by the post processing code are also indicated in Figure 4b. A mesh of rectangular elements whose nodes are located in the centres of patches has been selected. Four material points per element have been included. The deformed slope, defined by the post processing code, has been plotted using the accumulated displacements of material points, representing physical particles, calculated by means of the post-process procedure developed. Once PIV measurements are processed, displacements, velocities, accelerations and strains are available for each particle defined at each time step during the recorded motion.

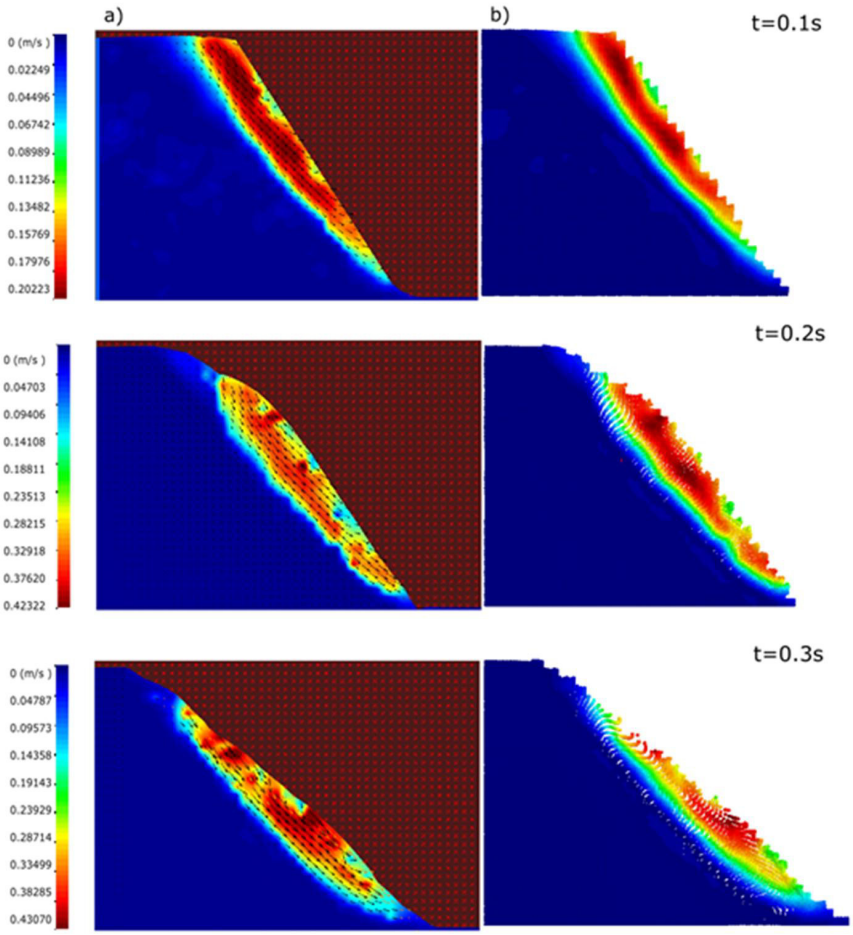

Fig. 4.Contours and vectors of velocities in m/s at different times (indicated in the figures). (a) Measured by means of PIV-Lab in the centres of patches and (b) reproduced by the post-processing code.

3.3. MPM simulation. Comparison between computed results and post-processed measurements

The slope failure has been simulated by means of the MPM code GeoPart[12],[13]. Results are compared with measurements with the aim of showing the usefulness of the methodology proposed to compare MPM numerical results with PIV measurements.

The sand is simulated as a one-phase material (dry soil) and a Mohr-Coulomb model was selected to define the constitutive behaviour. Properties of the sand introduced in the MPM calculated are indicated in Table 1. Sand density is measured as an average value taking into account the volume of the slope and the total weight of the material. The maximum and minimum density of the sand measured in the laboratory by a standard procedure (UNE 103-105-93) are 1795 kg/m^3 and 1442 kg/m^3, respectively. An average relative density of 28% is calculated for the sand used in the experiment.

Table 1. Sand properties.

Sand density	1540 kg/m³
Grain density	2665 kg/m³
Porosity	0.42
Poisson's coefficient	0.3
Young's modulus	30 MPa
Cohesion	0
Friction angle	43º

The sand was previously tested in a conventional direct shear test to evaluate the strength. A friction angle equal to 30º was measured in the range of 50-200 kPa of vertical stress and a nil value for cohesion was obtained. A higher friction angle (43º) has been considered in the MPM simulation which has been calibrated by back analysis to fit better the observed post-failure behaviour of the slope. An increment of the friction angle with respect to the value measured in the direct shear tests can be explained taking into account the level of the stress actually acting on the failure surface. The failure surface observed in the experiment is located at few centimetres deep which involves a vertical stress lower than 2 kPa. This value is close to two orders of magnitude lower than the stress applied in the laboratory tests where a friction angle equal to 30º was measured. Conventional shear box testing apparatus are no suitable to evaluate the properties of soils at low normal stresses because the error due to the internal friction of the apparatus became significant in the results [14][15]. It is known that the sand exhibits a non-linear strength increase with confining stress due to grain interlocking effects [15]. High friction angles in the range of 47º to 70º are reported in this reference, as well as strain softening effects, for confining stresses (triaxial experiments) of 0.05 to 1.3 kPa and relative densities of 65% - 85%. These results indicate that the operating sand friction in the 1g test performed should be substantially larger than the value measured in standard shear box tests. The back analysed friction by fitting MPM results is consistent with the mentioned data. Note also that the calculation code used does not consider the nonlinearity of the strength envelope expected at low confining stresses

The friction angle (43º) introduced in calculations coincides with the average slope angle of the final geometry in the upper part of the slope once the slope stabilizes after failure. This can be observed in Figure 5a where the final slope geometry is plotted once the equilibrium is restored. In the figure, two colours are selected to distinguish the material mobilized during the landslide with respect to the material that remains at rest. The slope angle of the material at rest is also equal to 43º. The final geometry can be compared with calculated results plotted in Figure 5b. The calculated volume of the material which did not move is similar to the volume observed in the experiment. On contrary, the final geometry of the mobilized material is not well captured because in the model sand accumulates in the central and upper parts of the slope which is a result not observed in the experiment.

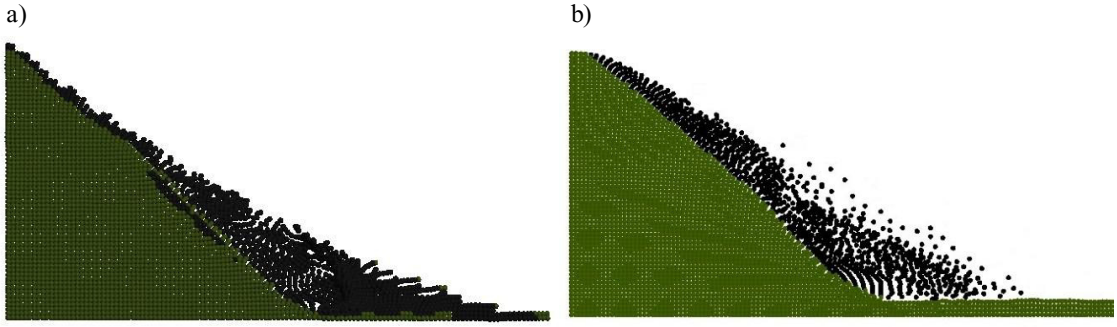

Fig. 5. Final geometry. The movilized material is indicated in black. Green colour indicates the material than remains at rest. (a) Post-processed PIV measurements. (b) MPM results.

Accumulated displacements and the equivalent plastic strains ($\varepsilon_{eq} = \sqrt{\left(\frac{2}{3}\mathrm{e}:\mathrm{e}\right)}$, where e is the deviatoric strain tensor) are plotted in Figures 6 and 7 at three different times. Post processed PIV measurements are compared with MPM numerical results. The calculated geometry of the mobilized mass match quite well the experimental measurements. The magnitude of the accumulated displacements is similar although higher values are calculated

near the slope surface when compared with experimental observations (Fig. 6). A unique shear band is observed in the experimental results whereas numerical calculation indicate that shear strains localize in two shear bands that are developed simultaneously (Fig. 7). This discrepancy is probably associated with the complex behaviour of sand at very low confining stresses (nonlinear strength envelope; strain softening behaviour) which are features not reproduced by the standard elastoplastic Mohr Coulomb model used. The equilibrated average sand slope in the experiment is 26º (measured in Figure 3b) which could be compared with calculated value of 31.5º in Figure 5b. Difficulties to match real boundary conditions at the lower part of the slope may also contribute to explain the discrepancies observed.

The PIV post-processing code allows plotting the evolution of selecting variables for each material point representing physical particles. For instance, the evolution of accumulated displacements at three material points is plotted in Fig. 8. Numerical results are compared with values calculated directly from PIV measurements once post-processed. The agreement is reasonably good.

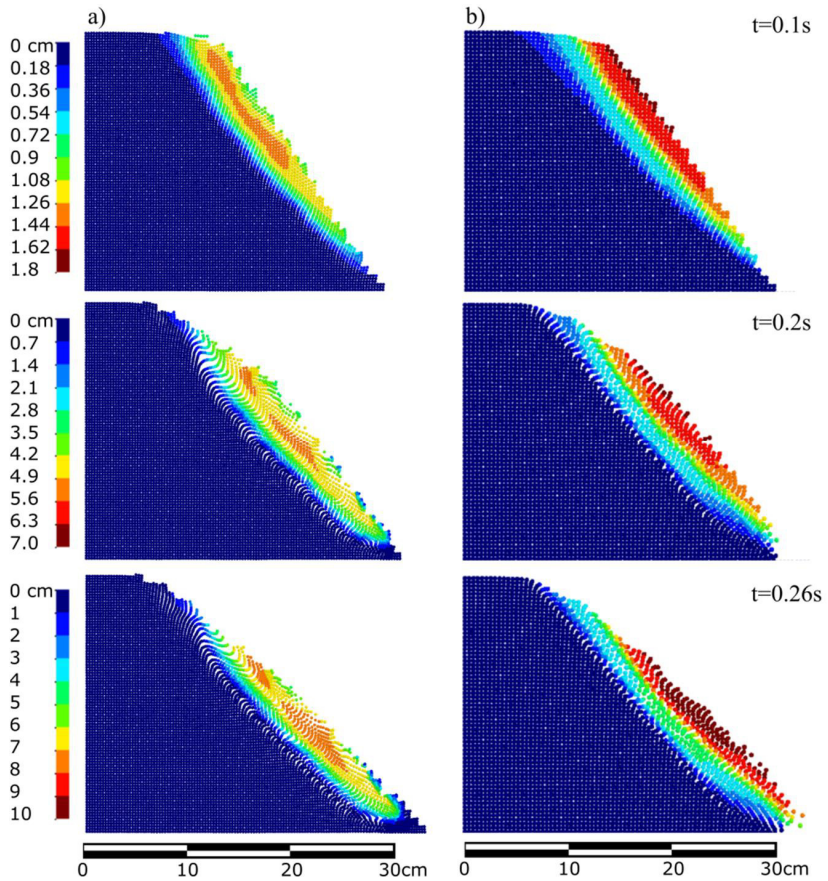

Fig. 6.Accumulated displacements for three different times. (a) Post processed PIV measurements and (b) MPM numerical results.

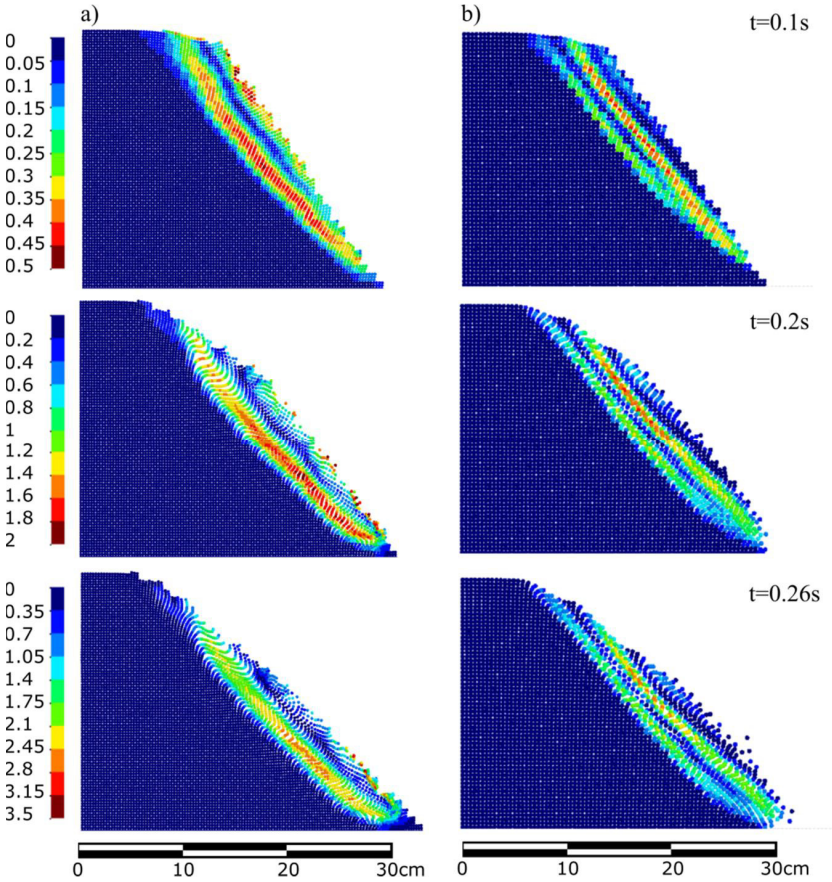

Fig. 7.Equivalent plastic strain. (a) Postprocessed PIV measurements and (b) MPM numerical results.

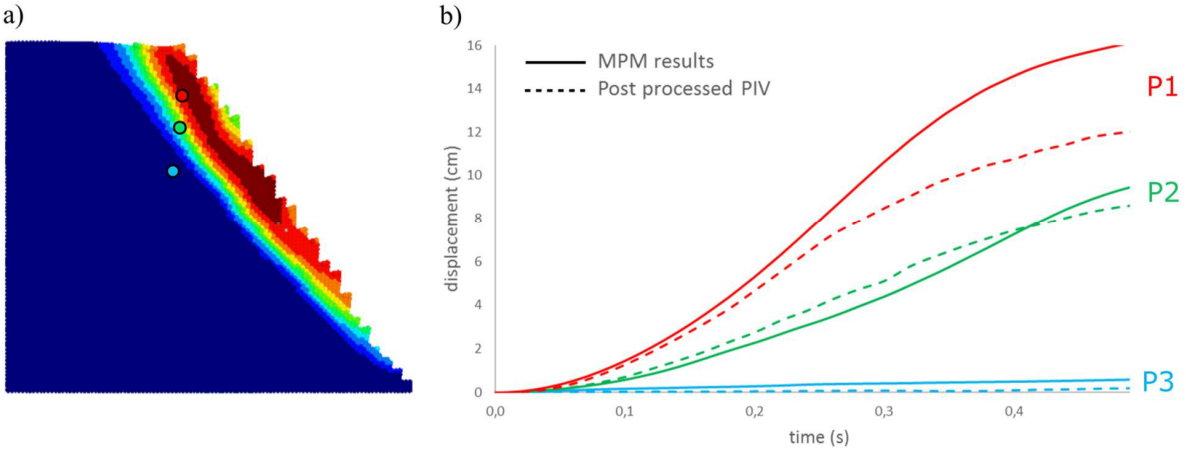

Fig. 8. Accumulated post-failure displacements of the slope. (a) Position of the three selected points; (b) Comparison of MPM results and experimental observations after being postprocessed.

4. Conclusions

The post-processing procedure described in this paper is a powerful tool to improve PIV techniques currently used in the interpretation of experiments involving large displacements. The method allows a direct validation of numerical tools such as the Material Point Method. The example described illustrates first the ability of the PIV post processing method developed to reproduce the observed deformation of a sand slope failed in a 1g experiment. The method provides also time records of displacements, velocities, accelerations and strain fields. These variables allow a direct comparison with MPM calculations, which is of special value in the exercise of validating MPM calculations. The paper describes also a comparison of the MPM modelling of the slope and the interpreted PIV measurements. Shearing behavior of sand at very low normal stresses typical of small scale 1g experiments is rather complex and this observation probably explains some discrepancies highlighted in the paper

References

[1] R. J. Adrian, Particle-imaging techniques for experimental fluid mechanics. Annual review of fluid mechanics, 23 (1991) 261-304.
[2] D. J. White, W. A. Take, M. D. Bolton, Soil deformation measurement using particle image velocimetry (PIV) and photogrammetry. Geotechnique, 53(7) (2003) 619-632.
[3] W. A. Take, M. D. Bolton, P. C. P. Wong, F. J. Yeung, Evaluation of landslide triggering mechanisms in model fill slopes. Landslides 1(3) (2004) 173-184.
[4] W. Take, M. D. Bolton, Identification of seasonal slope behaviour mechanisms from centrifuge case studies. Proceedings of the Conference on Advances in Geotechnical Engineering. Thomas Telford, (2004).
[5] M. Gilbert, F. W. Smith, J. Wang, P. A. Callaway, C. Melbourne. Small and large-scale experimental studies of soil-arch interaction in masonry bridges. In 5th International Conference on Arch Bridges ARCH (2007) (Vol. 7, pp. 381-388).
[6] M. Niedostatkiewicz, D. Lesniewska, J. Tejchman, Experimental analysis of shear zone patterns in cohesionless sand for earth pressure problems using particle image velocimetry. Strain, 47(s2), (2011) 218-231.
[7] C. Senatore. M. Wulfmeier, I. Vlahinić, J. Andrade, K. Iagnemma, Design and implementation of a particle image velocimetry method for analysis of running gear–soil interaction. Journal of Terramechanics 50(5) (2013). 311-326.
[8] B. Pan, K. Qian, H. Xie, A. Asundi, Two-dimensional digital image correlation for in-plane displacement and strain measurement: a review. Measurement science and technology, 20 (2009)062001, 17pp.
[9] W. A. Take. Advances in visualization of geotechnical processes through digital image correlation. Thirty-Sixth Canadian Geotechnical Colloquium. Canadian Geotechnical Journal 52(9) (2015) 1199-1220.
[10] N. M. Pinyol, M. Alvarado. Novel PIV-based analysis for large displacements. (2016). Canadian Geotechnical Journal. Submitted.
[11] W. Thielicke, E. J. Stamhuis. PIVlab–Towards user-friendly, affordable and accurate digital particle image velocimetry in MATLAB. Journal of Open Research Software 2(1) (2014) e30.
[12] F. Zabala, R. Rodari, L. Oldecop, Localización de deformaciones en estructuras geotécnicas utilizando el método del punto material. Revista Sul-americana de Engenharia Estrutural, 1(2). (2008).
[13] F. Zabala, E. E. Alonso, Progressive failure of Aznalcóllar dam using the material point method. *Géotechnique*, *61*(9). (2011). 795-808.
[14] B. M. Lehane, Q. B. Liu, Measurement of shearing characteristics of granular materials at low stress levels in a shear box. Geotechnical and Geological Engineering, (2013). 31(1), 329-336.
[15] S.Sture, C. Costes, S. N. Batiste, M. R. Lankton, K. A. AlShibli, B. Jeremic, R.A. Swanson, M. Frank. Mechanics of granular materials at low effective stresses. Journal of Aerospace Engineering, Vol., 11, No. 3, July, (1998). 67-72.